J. Fluid Mech. (1975), *vol.* 68, *part* 4, *pp.* 813–829
Printed in Great Britain

Search for the final period of decay of the axisymmetric turbulent wake

By PETER FREYMUTH

Department of Aerospace Engineering Sciences, University of Colorado, Boulder

(Received 15 January 1974)

Profiles of mean and fluctuating turbulent velocities and temperatures, of the time derivative of velocity and of intermittency have been measured in the wake of an unheated as well as a heated sphere in the low Reynolds number range 600–2500 at distances 80–1800 sphere diameters downstream. The wind-tunnel experiments exhibit a strong dependence on Reynolds number but they do not indicate the attainment of or an approach to the final period of turbulent decay which has been explored theoretically by Phillips and by O'Brien. The lowest turbulence Reynolds number obtained was $R_\lambda = 1{\cdot}4$.

1. Introduction

Linearization of the equations of fluid motion has a long tradition, especially for the axisymmetric wake. It goes back to Stokes (1851) for the laminar wake close to a sphere and it has been applied by Oseen (1910) to the far laminar wake behind bodies of revolution for higher Reynolds numbers. Linearization of the equations of turbulent motion was first introduced by von Kármán & Howarth (1938), for isotropic flow. Batchelor & Townsend (1948) considered this low Reynolds number approximation for homogeneous turbulent flow and coined the term 'final period of turbulent decay'. The asymptotic theory of Batchelor & Townsend has been extended by Phillips (1955) to the axisymmetric turbulent wake and it has been extended further by O'Brien (1973) to include the decay of turbulent scalar fields such as temperature. The theory of Saffmann (1967) for homogeneous turbulence should also be mentioned although it has not been extended to the axisymmetric wake.

Whereas the theoretical effort concerning the final period of turbulent decay is remarkable, experimental investigations into this subject are rare. Batchelor & Townsend (1948) found that grid turbulence at turbulence Reynolds numbers below 5 tends to support their theory. For the axisymmetric wake behind a disk Hwang & Baldwin (1966) mentioned possible attainment of the final period at a turbulence Reynolds number of 30, without, however, specifically comparing experimental and theoretical results. Waser (1971) reported an increase in spreading rate in the far wake behind a spheroid and he attributed this to the attainment of the final period of turbulent decay. Since the spreading of the wake in the final period is not aided by turbulent diffusion the spreading rate should however decrease with the attainment of the final period rather than increase.

There exists a group of flow-visualization experiments for wakes behind spheres and disks (adequately referenced by Willmarth, Hawk & Harvey 1964) which shows a laminar wake at low Reynolds numbers, a periodic wake at medium Reynolds numbers and a turbulent wake at higher Reynolds numbers. Although these experiments are not concerned with the final period they show that experiments concerning the final period cannot be performed below certain Reynolds numbers (of order several hundred).

Recently Achenbach (1974) found periodicity in the near wake of a sphere at Reynolds numbers as high as 3×10^5, as demonstrated by a peak in the one-dimensional power spectra. On the other hand, the numerous power spectra obtained by Uberoi & Freymuth (1970) and by Freymuth & Uberoi (1973) in the far turbulent wake of a sphere up to Reynolds numbers of $1{\cdot}5 \times 10^5$ do not exhibit a peak. It is therefore obvious that any periodicity in the wake close to the sphere decays rapidly and no trace of it can be found in the far wake. This result had already been obtained by Möller (1938) from flow-visualization experiments and is completely analogous to the subsequent findings by Roshko (1954) for the turbulent wake behind a cylinder. Most recently, De Coster & Kibens (1974) seem to have found some persistence of periodicity in the far wake behind a disk, indicating that a sphere wake is a more suitable choice for exploring the final period of turbulent decay.

Recently O'Brien (1973) compared some of his theoretical results with wind-tunnel measurements in the wake behind a heated sphere by Freymuth & Uberoi (1973). He found some qualitative agreement. These measurements were however, made at moderate rather than at low Reynolds numbers. Therefore an extension of these measurements to lower Reynolds numbers would lend a comparison more significance.

The purpose of this investigation is to assess how far the final period for the axisymmetric turbulent wake can be attained under laboratory conditions. The assessment will mainly be based on wind-tunnel measurements in the low Reynolds number turbulent wake behind a sphere and on a comparison of results with the theoretical predictions for the final period.

2. Experimental arrangement

The measurements were performed in a variable-speed (1–14 m/s) vertical wind tunnel built for our purposes with a test section $20{\cdot}3 \times 20{\cdot}3$ cm wide at the top and 2 m long (see figure 1). Two of the tunnel walls were adjustable in order to create a constant pressure flow in the test section. The turbulence level varied with speed and position in the tunnel but was typically of order

$$(\overline{u'^2})^{\frac{1}{2}}/U_0 = 0{\cdot}06\text{–}0{\cdot}08\,\%$$

for our measurements, where u' is the velocity fluctuation in the mean flow direction, U_0 is the free-stream velocity and a bar denotes an average. A turbulent axisymmetric wake was created by means of a steel sphere of diameter

$$D = 0{\cdot}397\text{ cm}.$$

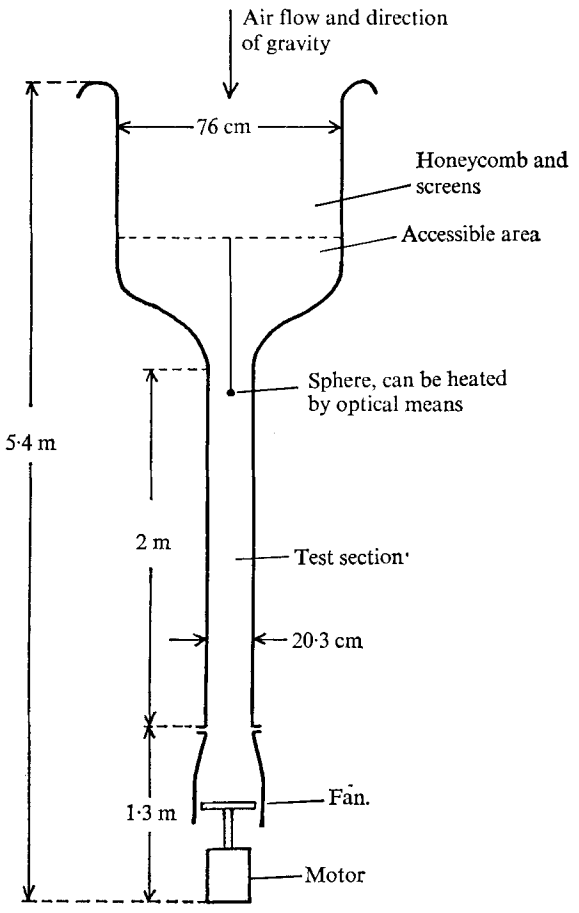

FIGURE 1. Wind-tunnel and sphere for creating an axisymmetric wake.

The sphere was suspended on a tungsten wire 0·002 cm in diameter into the upper part of the test section. Glass windows in the tunnel wall allowed the focusing of a light beam from a projector lamp on the blackened steel sphere as a means of heating the sphere.

During the wake experiments the sphere executed small irregular pendulum motions at an approximate frequency of 0·6 Hz with an amplitude not exceeding 0·2 sphere diameters. These small and slow motions were not expected to influence the wake measurements to any measurable degree since the wake width where measurements were performed was of order 15 sphere diameters or more. As a check some measurements of velocity fluctuations were performed for which the tunnel was started from rest. The tunnel reached equilibrium flow conditions within 20 s whereas the pendulum motions of the sphere reached their full amplitude not before a minute. The wake measurements had already reached equilibrium after 20 s, showing that the pendulum motions of the sphere had no influence.

In addition, spheres of different sizes yielded the same dimensionless profiles of temperature and velocity fluctuations at the same Reynolds number, although the amplitude of the pendulum motions as well as the spectral content of the velocity fluctuations in the wake changed with sphere size. This also shows the insignificance of the sphere motions.

Measurements of axial velocity fluctuations in the wake were made with low noise hot-wire equipment described by Freymuth (1967); the mean velocity dip in the wake was measured with a hot-wire anemometer having a low drift as described by Bank (1972). The free-stream velocity was monitored with a Pitot tube connected to a pressure transducer. The temperature and its fluctuations were measured by means of a resistance thermometer with a platinum–10% rhodium wire $6{\cdot}4 \times 10^{-5}$ cm thick and fed with a current of 0·25 mA. The wire length was 0·03 cm. The probes were mounted on a sliding bar that could be moved across the tunnel. Various downstream positions were obtained by exchanging 46 cm long cover plates for the tunnel with the plate containing the movable probes.

For data processing various filters, root-mean-square voltmeters, amplifiers, oscilloscopes and a constant bandwidth wave analyser were available.

3. Experimental results

3.1. *General remarks concerning the experiments*

The theories by Phillips (1955) and by O'Brien (1973) investigate an axisymmetric turbulent wake which is homogeneous in the axial direction and decays in time whereas the wake behind a sphere is homogeneous in time and decays in the axial direction. Intuitively results for these two different configurations can be related to each other by a Galilean transformation; it will be shown in the appendix that within the framework of an asymptotic theory of the final period this is indeed the case. Therefore results obtained in the sphere wake will be checked against the theories by Phillips and by O'Brien.

For the final period, O'Brien (1973) predicted profiles across the wake of the mean temperature excess ΔT over the ambient value and of the correlations $\overline{v'T'}$ and $\overline{v'T'^2}$, where T' is the temperature fluctuation and v' the radial velocity fluctuation at a point, which qualitatively agree with the profiles measured by Freymuth & Uberoi (1973) at rather high Reynolds numbers. For the mean-square temperature fluctuations $\overline{T'^2}$, however, a Gaussian profile was predicted for the final period whereas measurements at higher Reynolds numbers showed a two-maximum profile with a minimum at its centre. Analogous discrepancies were found for the mean-square axial velocity fluctuation $\overline{u'^2}$. According to a private communication from O'Brien profiles of $\overline{u'^2}$ predicted on the basis of Phillips' (1955) theory are nearly bell shaped whereas measurements by Uberoi & Freymuth (1970) showed two maxima. Another discrepancy between final-period theory and wake measurements at higher Reynolds numbers is the presence of intermittency in measurements in the outer parts of the wake and its absence in the asymptotic theories.

The measurements to be reported in this section concentrated on those quantities which showed the least agreement with the asymptotic theories and thus presumably offered the most sensitive criteria for the attainment of the final period. These quantities (profiles of temperature and velocity fluctuations across the wake and of the intermittency factor) presumably also exhibited the strongest dependence on Reynolds number. Measurements were started at fairly high Reynolds numbers; the Reynolds number then was gradually decreased to the minimum value for which a fully turbulent, non-periodic wake was still obtained.

Uberoi & Freymuth (1970) showed that for the high Reynolds number turbulent wake behind a sphere

$$R_\lambda \sim R_c^{\frac{1}{2}} = [R(D/x)^{\frac{1}{3}}]^{\frac{1}{2}}, \tag{1}$$

where

$$R_\lambda = \frac{(\overline{u'^2})^{\frac{1}{2}} U_0}{\nu} \left[\frac{\overline{u'^2}}{(\partial u'/\partial t)^2}\right]^{\frac{1}{2}}$$

is the turbulence Reynolds number, $R = U_0 D/\nu$ is the Reynolds number of the sphere, ν is the kinematic viscosity, t is time and x is the downstream distance from the sphere. The above relation shows that the turbulence Reynolds number can be lowered most effectively by lowering R whereas an increase in downstream distance will have a rather weak effect.

The asymptotic theories of the final period predict power laws of decay for various turbulent quantities. Since these decay laws contain an arbitrary virtual origin at least a few measured data on decay can always be fitted to any decay law by choosing an appropriate virtual origin. Therefore data on decay with downstream distance from the sphere will only be reported, and not used to assess the attainability of the final period.

3.2. *Phenomenology of the far wake*

Most measurements of the far wake were made 195 sphere diameters downstream. Tracing velocity fluctuations at this station using an oscilloscope shows the following qualitative wake properties. Below $R = 305$ the wake is laminar, between $R = 305$ and $R = 390$ the wake is periodic, while above $R = 390$ the wake starts to become turbulent although periodicity can still be recognized. Above $R = 600$ all periodicity has vanished, and the wake has become fully turbulent. This can be seen more clearly from the one-dimensional power spectra of axial velocity fluctuations $[E_u(k)/E_u(k = 0)]$ and of temperature fluctuations $[E_T(k)/E_T(k = 0)]$ at $R = 625$ shown in figure 2, where $k = 2\pi f/U_0$ is the wavenumber. These spectra do not show any prominence of a single frequency and the same holds at higher Reynolds numbers. Furthermore, the spectra do not exhibit an inertial subrange at $R = 625$.

3.3. *Temperature and velocity fluctuations*

Figure 3 shows profiles of the intermittency factor $\gamma_T(r/D)$ of the temperature fluctuations, where r is the radial distance from the wake axis, measured 195 sphere diameters downstream at three different Reynolds numbers. The intermittency factor γ_T of a temperature fluctuation signal as observed by means of a

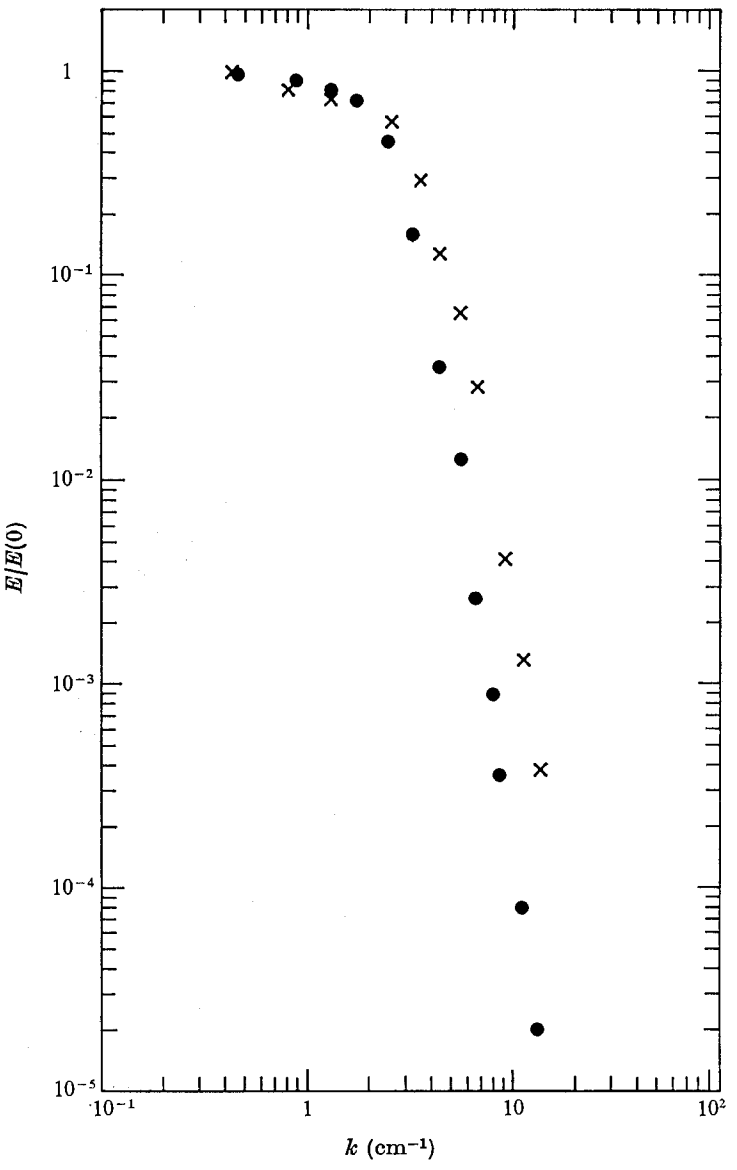

FIGURE 2. One-dimensional normalized power spectra of axial velocity fluctuations (circles) and of temperature fluctuations (crosses). $x/D = 195$, $R = 625$, $R_\lambda = 3{\cdot}4$, centre of the wake.

storage oscilloscope is the ratio of the time during which the signal is turbulent to the total time. Intermittency measurements based on this simple method have been compared by La Rue (1973) with results of more sophisticated methods of electronic measurement and found to be in good agreement. With decreasing Reynolds number the fully turbulent central region of the wake spreads to its outer regions. This brings the wake at low Reynolds number closer to the conditions assumed for the final period, at least as far as intermittency is concerned.

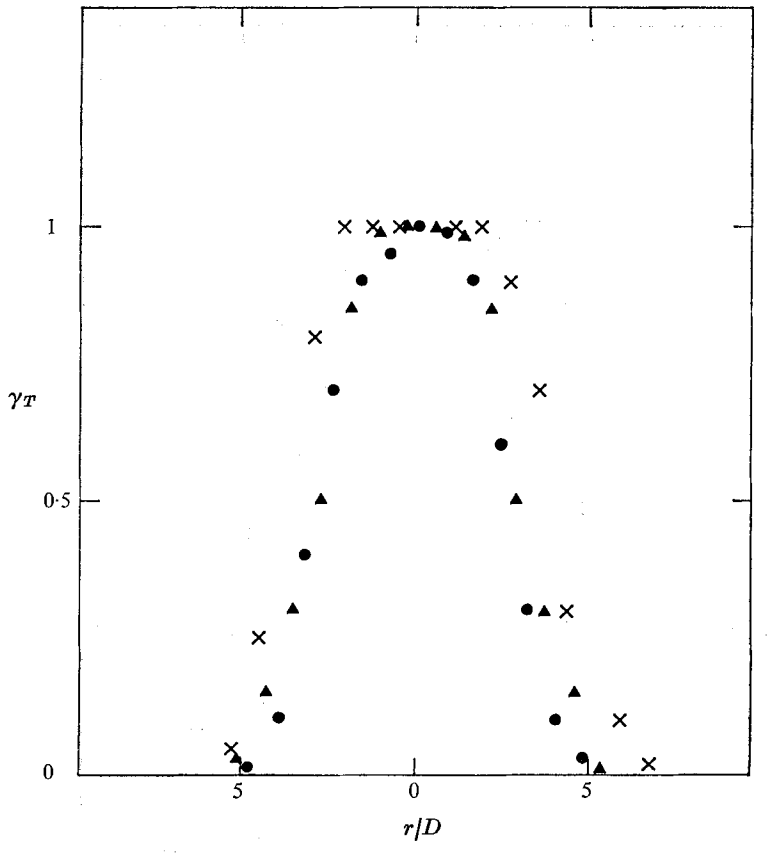

FIGURE 3. Profiles of intermittency factor γ_T. $x/D = 195$. ×, $R = 625$; ▲, $R = 1250$; ●, $R = 2500$.

Figure 4 shows normalized profiles of the temperature fluctuations

$$[\overline{T'^2}(r/D)/\overline{T'^2}(0)]^{\frac{1}{2}} \quad \text{at} \quad x/D = 195$$

for three different Reynolds numbers. It can be seen that with decreasing Reynolds number the two maxima in the profile become more prominent. This effect is opposite to what is needed to approach a bell shape with decreasing Reynolds number. The bell shape has been predicted by O'Brien (1973) for the final period. This effect did not depend on the degree of heating of the sphere and thus was not a buoyancy effect. It was even more dramatic for the fluctuations in axial velocity as shown in figure 5 for an entirely unheated sphere. In this figure a profile for the periodic–turbulent regime at $R = 485$ has also been included, showing that in this somewhat coherent flow regime the maxima become de-emphasized. Figures 4 and 5 also show the widening of the wake with decreasing Reynolds number.

Even profiles of time derivatives of velocity fluctuations, which usually have a rather flat maximum in the wake centre, acquire two maxima at low Reynolds numbers as is shown in figure 6.

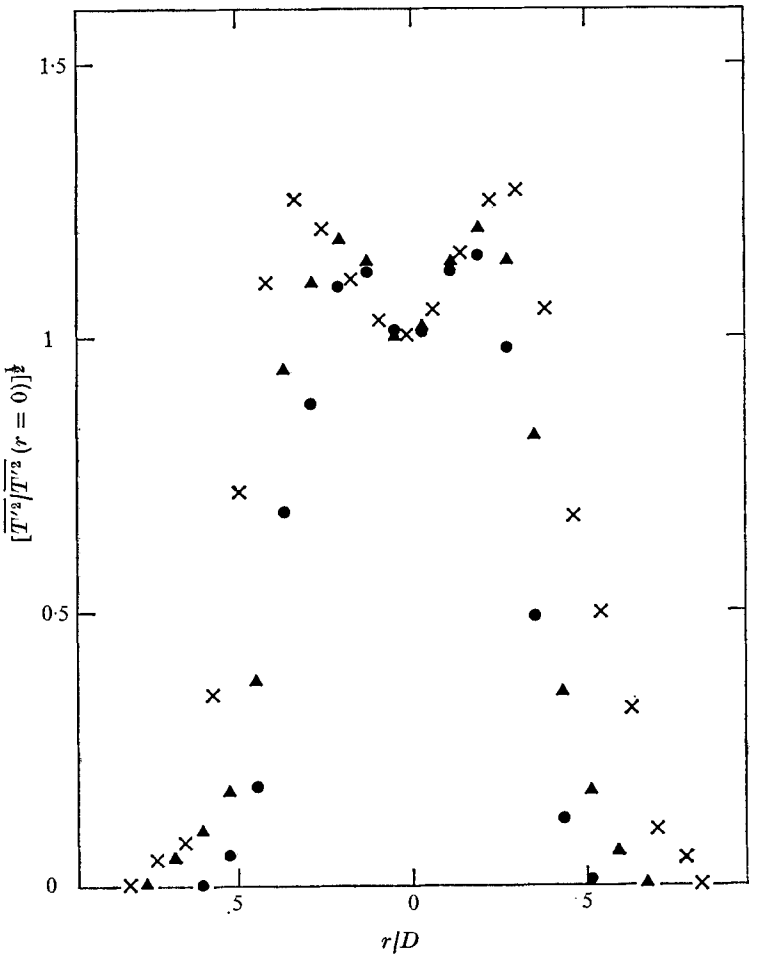

FIGURE 4. Profiles of normalized temperature fluctuations $[\overline{T'^2}/\overline{T'^2}(r=0)]^{\frac{1}{2}}$. $x/D = 195$. ×, $R = 625$, $R_\lambda = 3{\cdot}4$; ▲, $R = 1250$, $R_\lambda = 5{\cdot}2$; ●, $R = 2500$, $R_\lambda = 12{\cdot}7$. $[\overline{T'^2}(r=0)]^{\frac{1}{2}}$ of order 0·05 °C for all measurements.

The two maxima of the temperature and velocity fluctuations become slightly enhanced with increasing downstream distance x as can be seen from figure 7, where the ratios $[\overline{T'^2_{\max}}/\overline{T'^2}(r=0)]^{\frac{1}{2}}$ and $[\overline{u'^2_{\max}}/\overline{u'^2}(r=0)]^{\frac{1}{2}}$ are shown as functions of downstream distance x/D for $R = 625$. The units of the ordinate are arbitrary in order to accommodate the dependence of many different functions on x/D. Figure 7 also shows that velocity fluctuations decay in this low Reynolds number regime as $x^{-0{\cdot}8}$ whereas temperature fluctuations decay as $x^{-1{\cdot}1}$. It should be mentioned that the measurements of velocity fluctuations reported for $x/D = 1800$ were made in a large horizontal tunnel, and because of the rather small signals only show the general trend. Figure 7 also shows the decrease in the turbulence Reynolds number R_λ with downstream distance, with $R_\lambda = 1{\cdot}4$ at $x/D = 1800$.

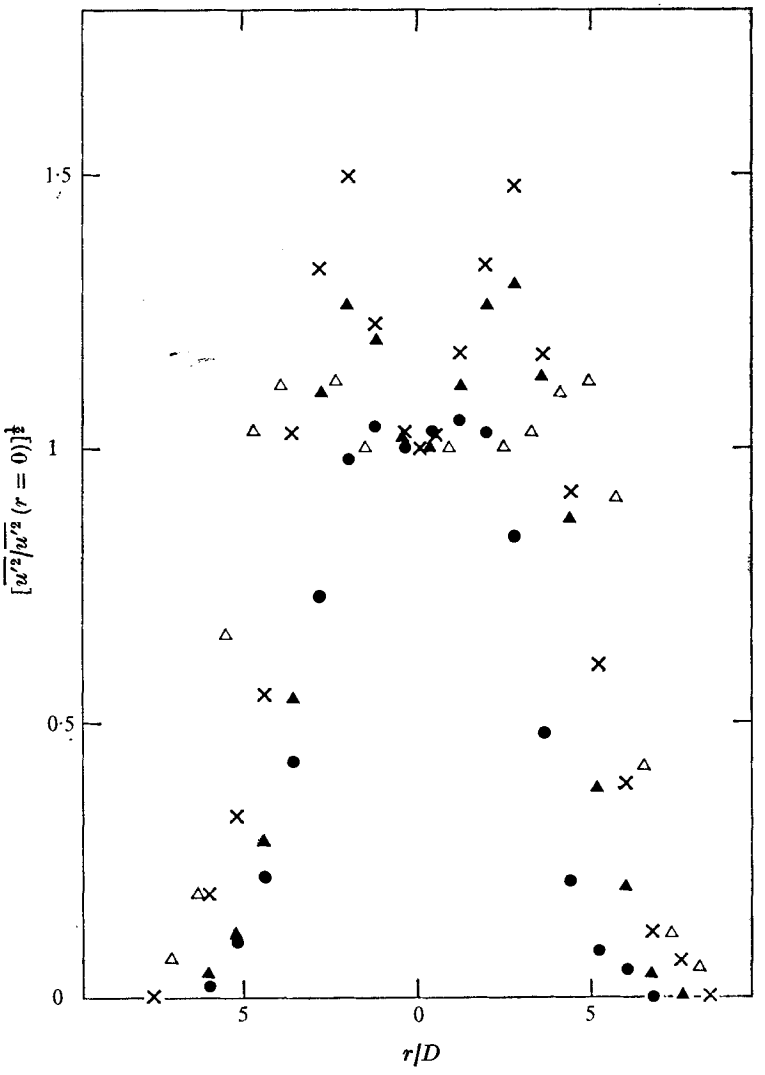

FIGURE 5. Profiles of normalized velocity fluctuations $[\overline{u'^2}/\overline{u'^2(0)}]^{\frac{1}{2}}$. $x/D = 195$. △, $R = 485$, $(\overline{u'^2(0)})^{\frac{1}{2}}/U_0 = 8{\cdot}3 \times 10^{-3}$; ×, $R = 625$, $(\overline{u'^2(0)})^{\frac{1}{2}}/U_0 = 3{\cdot}6 \times 10^{-3}$; ▲, $R = 1250$, $(\overline{u'^2(0)})^{\frac{1}{2}}/U_0 = 4{\cdot}1 \times 10^{-3}$; ●, $R = 2500$, $(\overline{u'^2(0)})^{\frac{1}{2}}/U_0 = 5{\cdot}5 \times 10^{-3}$. $U_0 = 6{\cdot}01$ m/s.

3.4. *Mean velocity and mean temperature*

Figures 4–6 show that the final period of turbulent decay as predicted by the asymptotic theories has neither been attained nor is it approached at a turbulence Reynolds number $R_\lambda = 3{\cdot}4$. Figure 7 gives no indication that the final period might be approached at even lower Reynolds numbers. This introduces the question whether the asymptotic state of the final period or whether the final period in general has not been reached. The final period in general requires that the turbulent transfer of momentum and heat in the wake be small compared with molecular transfer. Information on the relative magnitudes of these

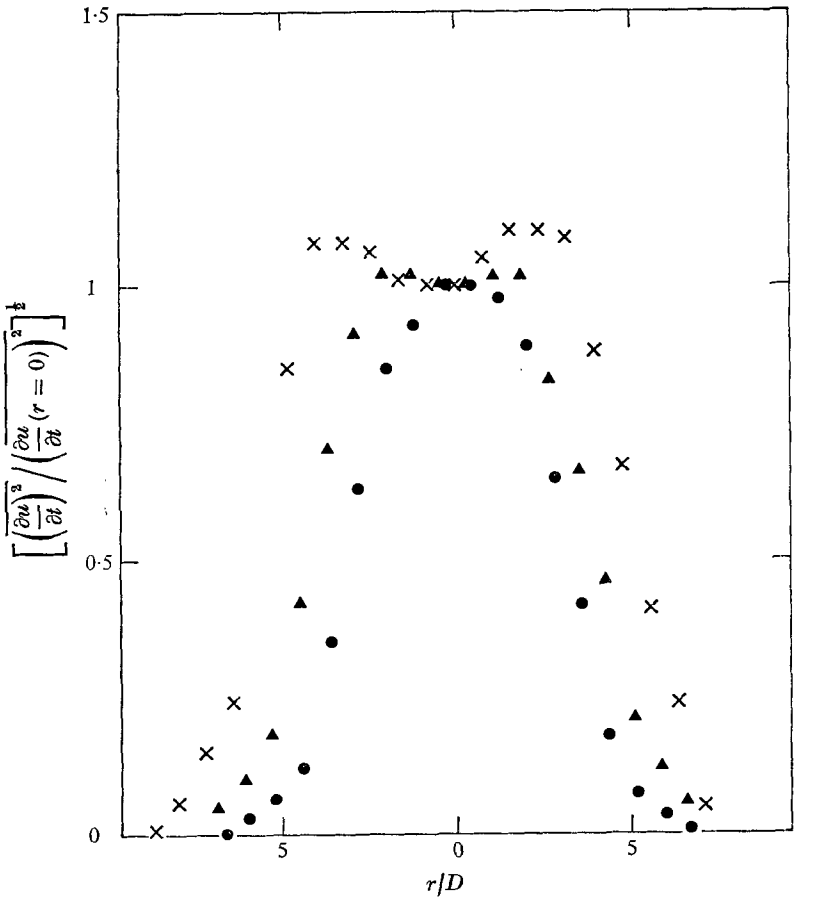

FIGURE 6. Profiles of normalized time derivative of velocity fluctuations

$$\left[\overline{\left(\frac{\partial u}{\partial t}\right)^2}\right]^{\frac{1}{2}} \Big/ \left[\overline{\left(\frac{\partial u}{\partial t}(0)\right)^2}\right]^{\frac{1}{2}}.$$

$x/D = 195$. ×, $R = 625$; ▲, $R = 1250$; ●, $R = 2500$.

quantities can be obtained from the mean temperature and velocity profiles and their decay with downstream distance.

Figures 8 and 9 show profiles of ΔT and of the mean velocity defect $\Delta U = U_0 - \overline{U}$ at various Reynolds numbers, where $\overline{U}$ is the mean velocity. Within the rather low measurement accuracy the profiles may be considered bell shaped. Figure 7 shows the decay of ΔT and ΔU and the increase in the half-width $b_{\frac{1}{2}}$ of the wake with increasing x for $R = 625$. Within measurement accuracy the wake decays according to $\Delta T \sim x^{-\frac{2}{3}}$, $\Delta U \sim x^{-\frac{2}{3}}$ and $b_{\frac{1}{2}} \sim x^{\frac{1}{3}}$, which are the decay laws found at high Reynolds numbers. On the basis of these decay laws it has been shown by Freymuth & Uberoi (1973) that the turbulent heat-transfer equation can be written as follows:

$$\frac{\overline{v'T'}}{\overline{U_c T_c}} = \frac{1}{3}\frac{r}{l_c}\frac{\Delta T}{T_c} + \frac{P}{R_c}\frac{d(\Delta T/T_c)}{d(r/l_c)}, \tag{2}$$

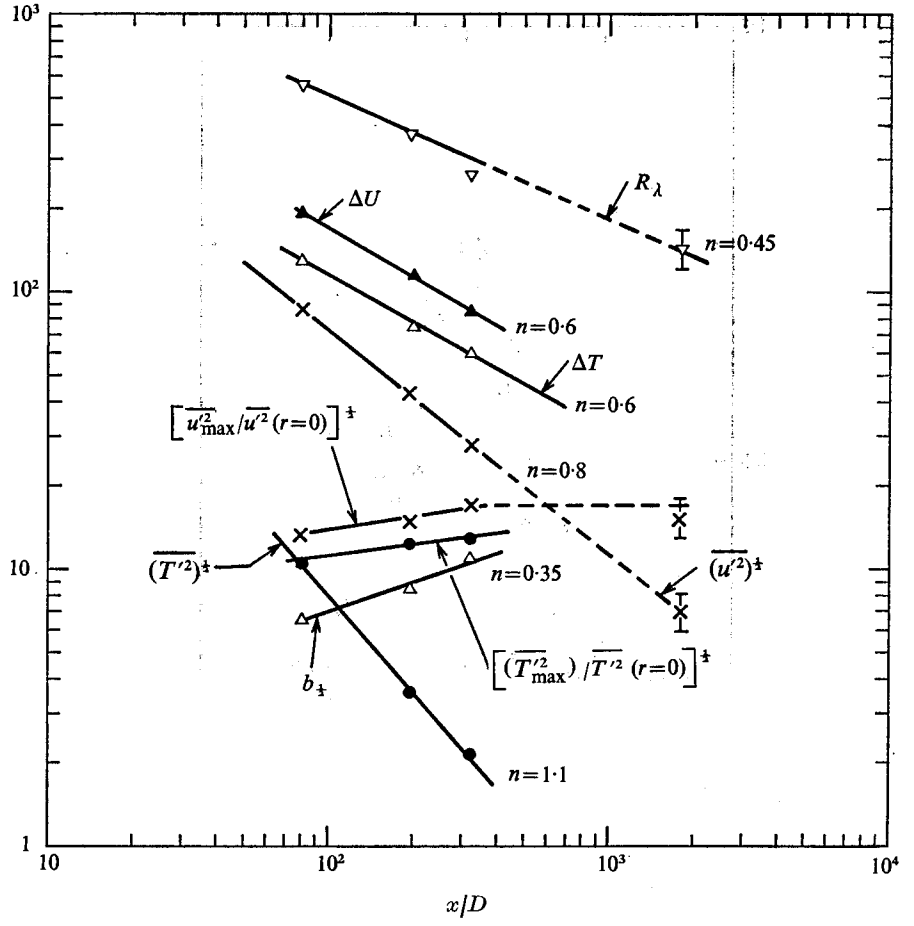

FIGURE 7. Dependence of various quantities on x/D. Ordinate scale is arbitrary. $R = 625$. n is the slope of the straight lines in this log–log representation.

where $U_c = U_0(D/x)^{\frac{2}{3}}$, $l_c = x^{\frac{1}{3}}D^{\frac{2}{3}}$, $R_c = U_c l_c/\nu = R(D/x)^{\frac{1}{3}}$, $T_c = \Delta T\,(r=0)$ and

$$P = \gamma/\nu = 1{\cdot}4 \text{ in air.}$$

Analogously the turbulent momentum equation reads

$$\frac{\overline{v'u'}}{U_c^2} = \frac{1}{3}\frac{r}{l_c}\frac{\Delta U}{U_c} + \frac{1}{R_c}\frac{d\Delta U/U_c}{dr/l_c}. \tag{3}$$

Assuming bell shapes for the temperature and velocity profiles, i.e.

$$\frac{\Delta T}{T_c} \sim \exp\left[-\kappa_1(r/l_c)^2\right], \quad \frac{\Delta U}{U_c} \sim \exp\left[-\kappa_2(r/l_c)^2\right],$$

where κ_1 and κ_2 are appropriate constants, it follows by means of (2) that the ratio r_T of turbulent to molecular heat transfer is given by

$$r_T = -\frac{\overline{v'T'}}{\gamma\,\partial(\Delta T)/\partial r} = \frac{1-6\kappa_1 P/R_c}{6\kappa_1 P/R_c} \tag{4}$$

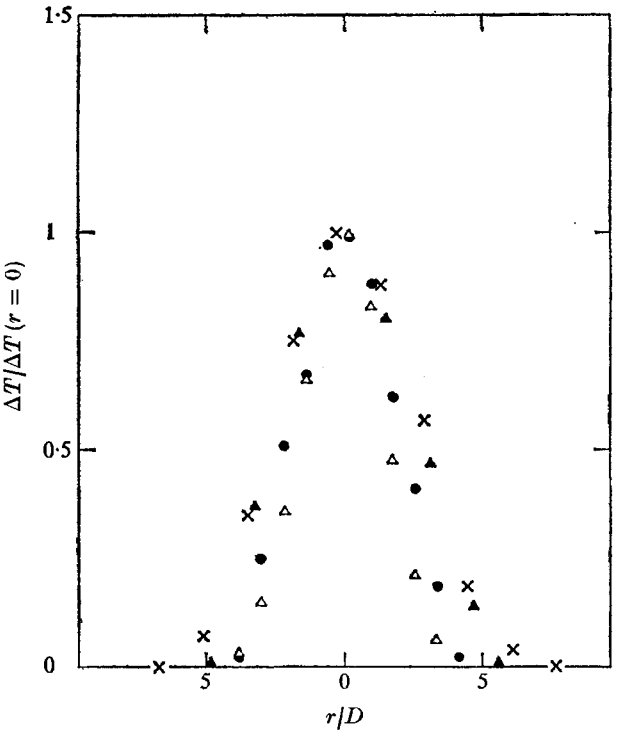

FIGURE 8. Profiles of normalized mean temperature over ambient $\Delta T/\Delta T(0)$ for various Reynolds numbers. $x/D = 195$. ×, $R = 266$ (laminar); ×, $R = 625$; ▲, $R = 1250$; ●, $R = 2500$.

and using (3) it follows that the ratio r_u of turbulent to molecular momentum transfer satisfies

$$r_u = -\frac{\overline{v'u'}}{\nu\,\partial(\Delta U)/\partial r} = \frac{1-6\kappa_2/R_c}{6\kappa_2/R_c}. \tag{5}$$

By means of figures 8 and 9 one finds that $\kappa_1 = 2{\cdot}5$ and $\kappa_2 = 3{\cdot}1$ at $R = 625$. As an example, the ratios r_T and r_u for $x/D = 195$ are $r_t = 4{\cdot}1$ and $r_u = 4{\cdot}8$; for $x/D = 1800$ one gets $r_T = 1{\cdot}4$ and $r_u = 1{\cdot}7$. The above results show that even far downstream the turbulent heat and momentum transfer are still larger than the molecular transfer. This means that the final period has not been reached. If the final period were reached further downstream the wake would still have to grow much wider by molecular diffusion in order to reach its asymptotic state (according to the asymptotic concept the initial state of the final period has to appear as a line source).

4. Final remarks

It has become apparent that our measurements do not approach the asymptotic values for the final period as the Reynolds number is decreased. Rather, differences between theory and experiments become more prominent although

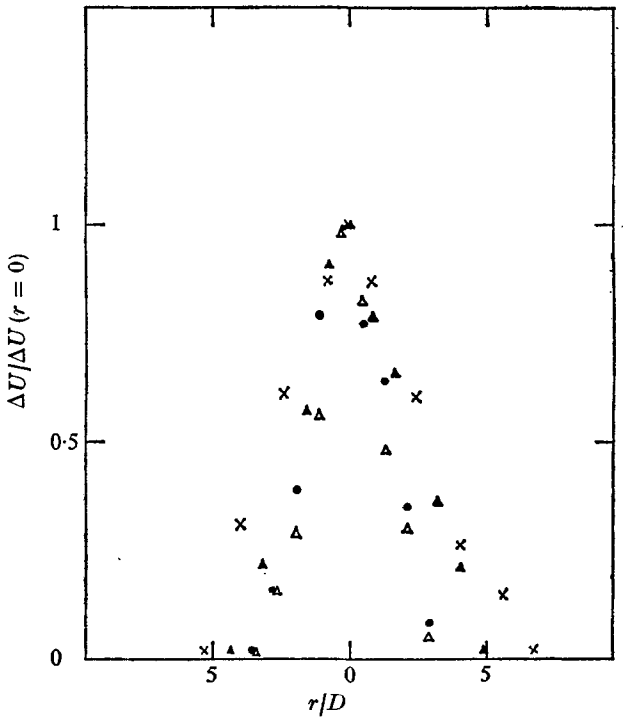

FIGURE 9. Profiles of normalized mean velocity defect $\Delta U/\Delta U(0)$. $x/D = 195$. △, $R = 266$, $\Delta U/U_0 = 57 \times 10^{-3}$; ×, $R = 625$, $\Delta U/U_0 = 12 \times 10^{-3}$; ▲, $R = 1250$, $\Delta U/U_0 = 7{\cdot}3 \times 10^{-3}$; ●, $R = 2500$, $\Delta U/U_0 = 8{\cdot}1 \times 10^{-3}$.

they might diminish at even lower Reynolds numbers. Unfortunately the Reynolds number cannot be decreased further in our experiments since the wake then becomes more and more periodic and finally laminar.

If the final period can be reached at all it seems that a barrier has to be overcome first. This can be seen more clearly from figure 10, where the half-width of the mean temperature profile is shown as function of Reynolds number. Approaching the laminar wake from right to left, a barrier has to be climbed before the widening turbulent wake collapses into a narrow laminar wake which may be considered a special case of the final period. The expected, direct approach path has also been drawn in the figure.

It should be mentioned that a few body shapes have been tried in addition to a sphere to create a low Reynolds number turbulent wake: a rod hanging into the test section of the tunnel and a streamlined body. The lowest turbulence Reynolds number in the wake behind these bodies was however larger by a factor 4 to 6 than that behind the sphere and thus these bodies were unsuited for an investigation.

It should be emphasized that the present investigation does not disprove the asymptotic theories. It only shows that it is hardly possible to verify the assumptions set forth in these theories under laboratory conditions. This is especially true for the velocity wake. For the temperature wake there exists the possibility

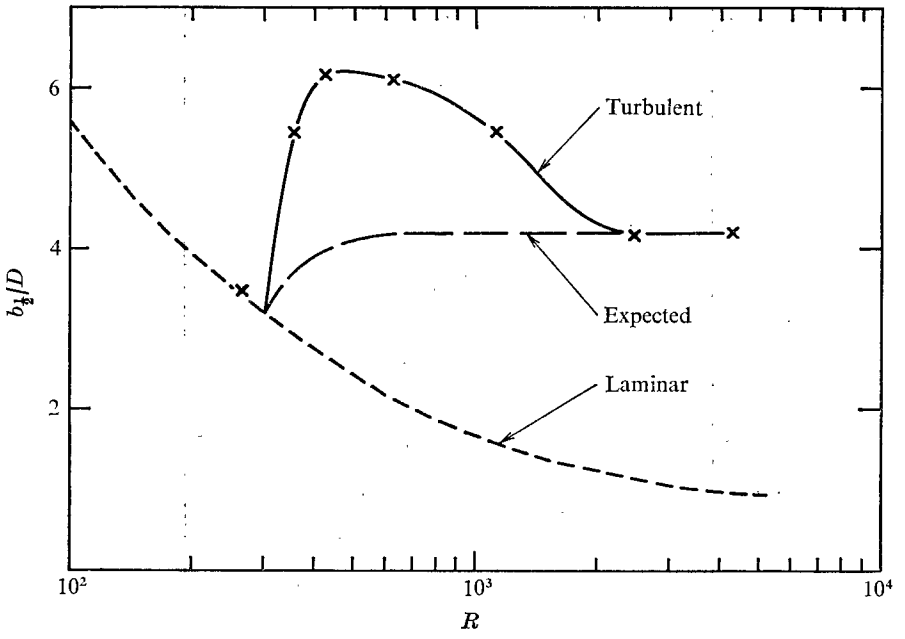

FIGURE 10. Dependence on Reynolds number of half-width $b_{\frac{1}{2}}$ of mean temperature profiles [width of wake where $\Delta T = \frac{1}{2}\Delta T(r = 0)$]. $x/D = 195$.

of using a fluid with small Prandtl number such as mercury and (owing to its high thermal diffusivity) forcing final-period conditions on the temperature wake even though the velocity wake has not reached that state. A mercury tunnel is not available to this author and formidable measuring problems might exist.

An axisymmetric body placed into a wind tunnel at sufficiently low Reynolds numbers creates a laminar wake. If the body is externally forced into random motions a pseudo-turbulent flow is generated. Such a flow should exhibit final-period behaviour if the random motions are kept sufficiently small. Experiments in this direction are under consideration.

Appendix

Temporal and spatial decay of turbulence

Let us consider two axisymmetric wake configurations in the final period one of which is homogeneous in the axial direction and decays in time t, the other being homogeneous in time and decaying in the axial direction x. For the axially homogeneous wake the mean flow is zero whereas for the temporally homogeneous wake the free-stream velocity U_0 in axial direction is large compared with the velocity defect of the wake. Asymptotic theories can be developed for both types of wake. It will be shown that for the profiles of mean and fluctuating temperature both theories are equivalent, i.e., they are connected by a Galilean transformation

$$x - x_0 = U_0(t - t_0), \tag{6}$$

where t_0 and x_0 are the virtual origins of the respective wakes. Let us consider the mean temperature profiles. The asymptotic theory yields for the temporally decaying wake (O'Brien 1973)

$$\Delta T \simeq \frac{1}{\gamma(t-t_0)} \exp\left[-\frac{r^2}{4\gamma(t-t_0)}\right]. \tag{7}$$

The mean heat-transfer equation for the axially decaying wake reads in the final period, when turbulent heat transfer is negligible,

$$U_0 \frac{\partial(\Delta T)}{\partial x} = \frac{\gamma}{r}\frac{\partial}{\partial r} r \frac{\partial(\Delta T)}{\partial r}, \tag{8}$$

which has the well-known asymptotic solution

$$\Delta T \simeq \frac{1}{\gamma(x-x_0)/U_0} \exp\left[-\frac{1}{4}\frac{r^2}{\gamma(x-x_0)/U_0}\right]. \tag{9}$$

Equations (7) and (9) are connected by the Galilean transformation (6) as predicted.

Let us next concentrate on the profiles of temperature fluctuations. For the temporally decaying wake O'Brien (1973) finds as asymptotic solution

$$\overline{T'^2} \simeq \frac{1}{[\gamma(t-t_0)]^{\frac{5}{2}}} \exp\left[-\frac{r^2}{2\gamma(t-t_0)}\right], \tag{10}$$

where the bar denotes an ensemble average. In order to obtain an analogous result for the axially decaying wake one has to find axially decaying elementary solutions for the temperature fluctuations and then synthesize the solution for the wake. In this we follow closely the procedure outlined by O'Brien (1973).

Denote by $T'(x, y, z, t)$ some temperature fluctuation in Cartesian co-ordinates for which there exists a Fourier transform $C(k_y, k_z, k_t, x)$ such that

$$T' = \int C(k_y, k_z, k_t, x) \exp\left[i(k_y y + k_z z + k_t t)\right] dk_y dk_z dk_t, \tag{11}$$

where k_y, k_z and k_t are the wavenumbers in the y and z directions and in time. The equation for temperature fluctuations in the final period reads

$$\frac{\partial T'}{\partial t} + U_0 \frac{\partial T'}{\partial x} - \gamma\left(\frac{\partial^2 T'}{\partial x^2} + \frac{\partial^2 T'}{\partial y^2} + \frac{\partial^2 T'}{\partial z^2}\right) = 0. \tag{12}$$

The corresponding equation for the Fourier transform is

$$\frac{\partial^2 C}{\partial x^2} - \frac{U_0}{\gamma}\frac{\partial C}{\partial x} - \left(k_y^2 + k_z^2 + \frac{ik_t}{\gamma}\right) C = 0. \tag{13}$$

Assuming an axially decaying solution of the form

$$C = C_0(x_0, k_y, k_z, k_t)\, e^{\alpha(x-x_0)} \tag{14}$$

yields for α

$$\alpha = \frac{U_0}{2\gamma} - \frac{U_0}{2\gamma}\left(1 + \frac{k_y^2 + k_z^2 + ik_t/\gamma}{(U_0/2\gamma)^2}\right)^{\frac{1}{2}}. \tag{15}$$

Developing α in a power series around the origin in wavenumber space and truncating after second-order terms yields as an elementary solution

$$C = C_0 \exp\left[-ik_t \frac{x-x_0}{U_0} - \left(k_y^2 + k_z^2 + \frac{k_t^2}{U_0^2}\right)\gamma \frac{(x-x_0)}{U_0}\right]. \tag{16}$$

C_0 can be considered as constant for asymptotically large x and we obtain as an elementary solution for T'

$$T' \simeq C_0 \frac{1}{[\gamma(x-x_0)]^{\frac{1}{2}}/U_0} \exp\left(-[y^2+z^2+\{U_0 t-(x-x_0)\}^2]\Big/\frac{4\gamma(x-x_0)}{U_0}\right). \quad (17)$$

The temperature fluctuation field in the axially decaying wake will be synthesized from solutions of the form (17) such that

$$T' \simeq \frac{1}{[\gamma(x-x_0)/U_0]^{\frac{3}{2}}} \exp\left(-\frac{r^2}{4\gamma(x-x_0)/U_0}\right) \int C(\tau) \exp\left(-\frac{[U_0(t-\tau)-(x-x_0)]^2}{4\gamma(x-x_0)/U_0}\right) d\tau. \quad (18)$$

For the ensemble average we therefore get

$$\overline{T'^2} \simeq \frac{1}{[\gamma(x-x_0)/U_0]^3} \exp\left(-\frac{r^2}{2\gamma(x-x_0)/U_0}\right) \times \int \overline{C(\tau)\,C(\tau')} \exp\left(-\frac{[U_0(t-\tau)-(x-x_0)]^2+[U_0(t-\tau')-(x-x_0)]^2}{4\gamma(x-x_0)/U_0}\right) d\tau\, d\tau'. \quad (19)$$

Assuming homogeneity in time, it follows that $\overline{C(\tau)\,C(\tau')}$ is a function of $\tau-\tau'$ only, or

$$C(\tau)\,C(\tau') = h(\sigma), \quad \text{where} \quad \sigma = U_0(\tau-\tau').$$

Introducing $\eta = U_0(t-\tau)-(x-x_0)$ yields

$$\overline{T'^2} \simeq \frac{1}{[\gamma(x-x_0)/U_0]^3} \exp\left(-\frac{r^2}{2\gamma(x-x_0)/U_0}\right) \int h(\sigma) \exp\left(-\frac{\eta^2+(\sigma+\eta)^2}{4\gamma(x-x_0)/U_0}\right) d\eta\, d\sigma. \quad (20)$$

Integration with respect to η yields

$$\overline{T'^2} \simeq \frac{1}{[\gamma(x-x_0)/U_0]^{\frac{5}{2}}} \exp\left(-\frac{r^2}{2\gamma(x-x_0)/U_0}\right) \int h(\sigma) \exp\left(-\frac{\sigma^2}{8\gamma(x-x_0)/U_0}\right) d\sigma. \quad (21)$$

For asymptotically large values of x the exponential function under the integral sign assumes the value one and in this case we get

$$\overline{T'^2} \simeq \frac{1}{[\gamma(x-x_0)/U_0]^{\frac{3}{2}}} \exp\left(-\frac{r^2}{2\gamma(x-x_0)/U_0}\right). \quad (22)$$

The above solution for axial decay is connected to the solution (10) for temporal decay by a Galilean transformation, as predicted.

Let us finally apply the theory of axial decay to calculate profiles of the temporal derivative of temperature fluctuations, which has not yet been done. Differentiating (18) with respect to t, squaring and averaging yields

$$\overline{\left(\frac{\partial T'}{\partial t}\right)^2} \simeq \frac{1}{[\gamma(x-x_0)/U_0]^3} \exp\left(-\frac{r^2}{2\gamma(x-x_0)/U_0}\right) \times \int \overline{C(\tau)\,C(\tau')} \exp\left(-\frac{[U_0(t-\tau)-(x-x_0)]^2+[U_0(t-\tau')-(x-x_0)]^2}{4\gamma(x-x_0)/U_0}\right) \times \frac{[U_0(t-\tau)-(x-x_0)]}{\gamma(x-x_0)/U_0} \frac{[U_0(t-\tau')-(x-x_0)]}{\gamma(x-x_0)/U_0} d\tau\, d\tau'. \quad (23)$$

Integration analogous to that for (20) yields

$$\overline{\left(\frac{\partial T'}{\partial t}\right)^2} \simeq \frac{1}{[\gamma(x-x_0)]^{\frac{7}{2}}} \exp\left(-\frac{r^2}{2\gamma(x-x_0)/U_0}\right), \tag{24}$$

which again is a bell-shaped profile. A similar shape might be expected for the derivative of the axial velocity fluctuations.

REFERENCES

ACHENBACH, E. 1974 *J. Fluid Mech.* **62**, 209.

BANK, W. 1972 *August E.D.N.* **15**, 43.

BATCHELOR, G. K. & TOWNSEND, A. A. 1948 *Proc. Roy. Soc.* A **194**, 527.

DE COSTER, M. A. & KIBENS, V. 1974 *Dept. Aerospace Engng, University of Michigan, Tech. Rep.* no. 012413.

FREYMUTH, P. 1967 *Rev. Sci. Instrum.* **38**, 677.

FREYMUTH, P. & UBEROI, M. S. 1973 *Phys. Fluids*, **16**, 161.

HWANG, N. H. C. & BALDWIN, L. V. 1966 *Trans. A.S.M.E.* **88**, 261.

KÁRMÁN, T. VON & HOWARTH, L. 1938 *Proc. Roy. Soc.* A **164**, 192.

LA RUE, J. C. 1973 Ph.D. thesis, University of California, San Diego.

MÖLLER, W. 1938 *Phys. Z.* **39**, 57.

O'BRIEN, E. E. 1973 *J. Fluid Mech.* **59**, 433.

OSEEN, C. W. 1910 *Ark. Mat. Astr. Fys.* **6**, 29.

PHILLIPS, O. M. 1955 *Proc. Camb. Phil. Soc.* **52**, 135.

ROSHKO, A. 1954 *N.A.C.A. Rep.* no. 1191.

SAFFMAN, P. G. 1967 *J. Fluid Mech.* **27**, 581.

STOKES, G. G. 1851 *Trans. Camb. Phil. Soc.* **9**, 8.

UBEROI, M. S. & FREYMUTH, P. 1970 *Phys. Fluids*, **13**, 2205.

WASER, R. H. 1971 *Turbulence in Liquids, Proc.*, p. 181.

WILLMARTH, W. W., HAWK, N. E. & HARVEY, R. L. 1964 *Phys. Fluids*, **7**, 197.